DRONEE: Dual-Radio Opportunistic Networking for Energy Efficiency

Arash Asadi*, Vincenzo Mancuso

IMDEA Networks Institute and University Carlos III of Madrid, Spain

Abstract

Reducing the power consumption of smartphones is becoming more and more important as smartphones become an indispensable component of our daily activities. In this work, we propose a novel scheme, so called DRONEE, that dramatically ameliorates energy efficiency for uplink transmissions, while achieving near-optimal throughput and high fairness levels in cellular networks. Our proposal consists in a novel two-tier uplink forwarding scheme in which users cooperate by forming clusters of dual-radio mobiles for hybrid wireless networks. The impact of our proposal is threefold: (*i*) energy efficiency is boosted by allowing mobiles to relay the cellular traffic through intra-cluster ad-hoc communications, which leads to reduction of power-hungry cellular transmissions; (*ii*) cellular capacity is augmented by scheduling uplink transmissions from mobiles with the best channel; (*iii*) almost perfect fairness is achieved by allowing users to share the cellular resources within their cluster. We corroborate the practical relevance of our proposal by providing a first-order discussion on the implementability of DRONEE using LTE and WiFi Direct.

Keywords: LTE, WiFi Direct, Device to Device (D2D), cooperative communications, hybrid networks, opportunistic scheduling

1. Introduction

In the past decade, the advent of smartphones and wireless broadband technologies has changed our daily habits and hobbies. Nowadays, people use smartphones for entertainment (e.g., chatting, reading news, social networking, and gaming) and work (e.g., email, stock market, etc.). Such a wide range of usage has stressed mobile operator's networks and smartphone's battery life. New smartphones come with high power processors and support simultaneous WiFi and cellular data connectivity, which drains batteries fast. Moreover, 3/4G cellular data technologies (i.e., LTE and LTE-A) are more power consuming than the previous generations. Since smartphone's battery life is limited, solutions leading to high energy efficiency are of utmost importance.

Prior works on energy efficiency in cellular data networks mostly proposed techniques such as traffic batching [1, 2] and traffic pattern learning [3]. These techniques are meant to increase the periods during which mobiles can switch off their wireless interfaces. There are also proposals to delay data transmissions until there is an opportunity to offload the data to a WiFi network [4, 5]. Existing proposals suffer from two drawbacks: (*i*) the extra delay introduced in the system, which makes them impractical for real-time and non-elastic services; and (*ii*) the complexity imposed to estimate future traffic patterns or to aggregate traffic from different applications. Moreover, existing proposals do not leverage the possibility to use more than one wireless interface at a time to *improve energy efficiency*. Some proposals do make use of multi-radio to improve performance, but they are not fully opportunistic and rather focus on coordinating multiple parallel connections for load balancing, P2P applications, multiplayer gaming, and multicast transmissions [6].

In contrast, in this article, we propose DRONEE (Dual-Radio Opportunistic Networking for Energy Efficiency), a novel scheme which fully leverages real-time cooperation of dual-radio devices with opportunistic scheduling for hybrid networks (i.e., using LTE and WiFi).

Using DRONEE, energy efficiency benefits from the opportunity to use mobiles to relay cellular traffic by means of WiFi. Specifically, LTE is used only for the data transmission of mobiles that have the top channel quality. Those mobiles act as a relay for the remaining nodes organized in clusters, as depicted in Figure 1. Differently from relay nodes, the other mobiles in the cellular network only use WiFi, which is much

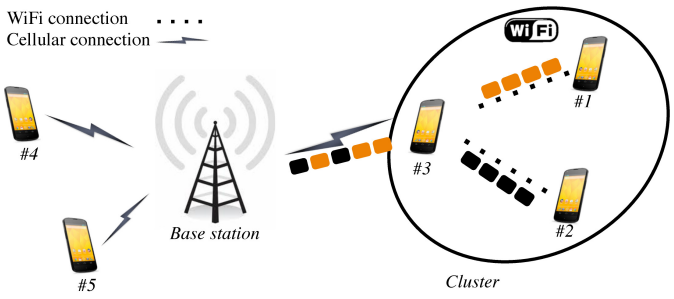

Figure 1: An example of a cellular network with clusters of dual-radio mobiles. Users 1 and 2 transmit their packets (which are colored in orange and black, respectively) over the WiFi network to the cluster head (i.e., User 3). Next, the cluster head forwards the packets to the base station.

*Corresponding Author: Arash Asadi; Address: Avenida del Mar Mediterraneo, 22, Leganes (Madrid), 28918 Spain; Phone: +34 91 481 6958; Fax: +34 91 481 6965.

Email addresses: arash.asadi@imdea.org (Arash Asadi), vincenzo.mancuso@imdea.org (Vincenzo Mancuso)

less energy consuming than LTE [7], to move their packets to and from relay nodes. Using an opportunistic scheduling strategy to select relay nodes results in enhanced energy efficiency while simplifying the scheduling tasks of the base station. Interestingly, DRONEE improves network throughput and fairness as well, without incurring the high complexity required by other technologies such as beamforming and MIMO. *Overall, DRONEE allows cellular users to enjoy seamless connectivity while spending more time on the WiFi interface, which is less power consuming than LTE, and switch off their LTE interface for long periods during which the LTE user channel's quality is not the strongest.*

This manuscript focuses on uplink transmission issues only, since the uplink represents the current technology bottleneck for transmission capacity, and transmission consumes more battery rather than reception. However, most of our proposal could be easily extended to downlink as well. The main contributions of this article are as follows: (*i*) in DRONEE, an architecture is proposed which exploits smartphone's multi-radio interfaces (i.e., LTE and WiFi) to *seamlessly improve* the energy efficiency of real-time cellular uplink operations; (*ii*) we propose and analyze a novel clustering scheme for heterogeneous users, which is part of DRONEE, and which adopts opportunistic and dynamic cluster head selection; (*iii*) we provide the first analytic model for power consumption of dual-radio mobiles in LTE-WiFi hybrid networks accounting for power saving features of LTE and WiFi; (*iv*) via extensive numerical simulation, we provide a performance evaluation of DRONEE, in terms of energy efficiency, throughput, and fairness in single-cell and multiple cell scenarios; (*v*) we discuss the implementation requirement and practicality of DRONEE in a real world system using LTE and WiFi Direct specifications.

The remainder of this manuscript is organized as follows. Section 2 discusses the related work. The system model is presented in Section 3. Section 4 numerically evaluates the clustering gain in single-cell and multi-cell scenarios. Section 5 provides a first-order discussion on the implementation feasibility of our proposal. Section 6 summarizes our findings and concludes the article.

2. Related Work

Although energy efficiency and wireless relay schemes have been proposed and extensively studied, there is little or no literature on jointly leveraging multi-radio, power saving capabilities of smartphones, and opportunistic scheduling to improve energy efficiency of uplink communications in cellular networks.

Energy efficiency. Cellular standards allow user equipment to switch off the transmission circuitry temporarily in order to save power. The majority of the proposals focus on leveraging this power saving option to reduce the active time of wireless interfaces. For instance, in [8], the authors analytically model power consumption of cellular mobile users and base stations, and illustrate the significance of continuous connectivity in power saving of mobile users. The authors also show how to optimize the power saving parameters to reduce the power consumption of mobile devices. However, [8] does not propose novel transmission schemes and does not consider capacity issues. Realistic models for the power consumption of mobiles have been proposed for LTE and WiFi in [9] and [10], respectively. The proposed models are desirable for two virtues: (*i*) they include the baseline power required to keep the interface up and running; (*ii*) they account for the variability of power consumption with transmission rate, while differentiating the cost of transmission from reception. However, these models do not account for power saving operations. In our proposal, we build on top of such models in order to provide a novel and more accurate model for power consumptions of wireless devices. Moreover, LTE and WiFi power consumption models are combined into a single generalized model for dual-radio devices.

The authors of [1] studied energy consumption in 3G and GSM networks. Their measurements reveal that a significant amount of energy is wasted when the wireless interface is still active but there is no data for transmission (i.e., *tail energy*). They propose an application layer protocol, namely *TailEnder*, that reduces the energy wasted in *tails* by delaying delay-tolerant data. Using a similar approach, Liu *et al.* [2] propose *TailTheft* which attempts to aggregate traffic of different applications to reduce the amount of the tail energy. Deng *et al.* [3] use a different approach by predicting traffic patterns to decide about active or idle state transitions. Differently from [1, 2, 3], our proposal only requires the use of standard defined power saving operations, while it does not require traffic coalescing, thus not incurring an excessive packet delay. The authors of [4, 5] address the fact that WiFi transmissions require less energy than 3G/LTE transmissions. Hence, they propose to delay the cellular traffic until a WiFi access point is available for offloading. Their approach induces significant delays and is only applicable to highly delay-tolerant applications. In contrast, our proposal does not need WiFi access points and induces negligible per-packet delay.

Wireless relay. The authors of [11, 12] propose to form clusters among mobile users with single antenna to emulate a MIMO device. Such an architecture requires precise synchronization between cluster members. Moreover, all cluster members have to maintain active and power expensive connections to the base station. Furthermore, Dohler *et al.* [12] proposed to use a secondary wireless interface (e.g., Bluetooth or WiFi) for coordinating MIMO operations. Yu *et al.* [13] propose Device-to-Device (D2D) communications in cellular networks for local traffic handling. D2D transmissions are meant to handle communications among two mobile devices, however, users do not help each other to relay traffic to the base station. Also, all transmissions occur over the same interface as cellular communications, and D2D resources are allocated by the base station.

Our extensive literature review indicates that none of the prior works categorized under packet forwarding, relaying, cooperative networks, and hierarchal clustering have the characteristics of our proposal, which are: (*i*) parallel use of multiple wireless interfaces (i.e., LTE and WiFi); (*ii*) clustering of wireless cellular devices; (*iii*) opportunistic cluster head selection; (*iv*) seamless connectivity with real-time cluster operations; and

(v) increase power saving opportunities, and thus energy efficiency, while achieving high cellular throughput and fairness.

3. DRONEE System Model

In order to boost energy efficiency and to make channel utilization more efficient in LTE cellular networks, we propose DRONEE, using a novel paradigm to leverage clusters of mobile users. In our clusters, *cluster heads* relay the cellular traffic generated within the clusters towards the base station (eNB in the LTE terminology), as shown in Figure 1.

With DRONEE, LTE mobile users form clusters by exploiting their secondary wireless interface, i.e., WiFi. Clusters form when the WiFi connectivity between cluster members is good, i.e., WiFi data rates are higher than the load generated in the LTE uplink by the cluster members. Among cluster members, only one node is allowed to transmit to the eNB, i.e., the *cluster head*. Differently from existing clustering schemes for sensor and vehicular networks [14, 15, 16], we propose to select the cluster head as the cluster member with the highest cellular channel quality at a given scheduling epoch. Therefore, a notable resource utilization increment stems from opportunistically and timely selecting cluster heads, based on the quality of their uplink LTE channels. Note that, with our proposal, scheduling of users is replaced with the selection of cluster heads. In particular, two possible cluster head selection and scheduling schemes will be discussed and analyzed in the remainder of this section, while the set of network procedures needed to implement DRONEE will be discussed in Section 5.

In what follows, we first present our model assumptions, and then it is shown how to compute the throughput of a cellular user i, namely $E[T_i]$, and its power consumption, denoted by $W_{tot}^{(i)}$, when DRONEE is adopted. In the numerical evaluation presented later in Section 4, the energy efficiency η of a user i will be computed as the quantity $E[T_i]/W_{tot}^{(i)}$.

3.1. Model Assumptions

We model uplink transmissions in an LTE-like [17] network operated by a single operator, with N cellular users generating uplink traffic. In our work, it is assumed that uplink resources S_{tot} are fixed for each scheduling epoch (frame), and users always have packets to transmit so that the network performance is evaluated under fully backlogged traffic conditions. In our analysis, the whole uplink frame resources S_{tot} are allocated to data transmission and a scheduled frame is allocated to one LTE transmitter only. The scheduled LTE transmitter is a cluster head, which is the mobile experiencing the best channel quality in its cluster. The cluster head is selected to connect to the base station on a per-frame basis. Therefore, the adopted scheduling strategy is channel-opportunistic. It is assumed that the base station is aware of cluster formation, so that it can allocate resources to cluster heads only. We will introduce the details of two possible opportunistic cluster head selection and scheduling schemes in Section 3.2.

The uplink LTE channel between mobile user i and the base station is characterized by stationary Rayleigh fading. Assuming that the SNR of user i is a random variable Γ_i with mean value γ_i, the CDF of the SNR has the following expressions:

$$F_i(z) = 1 - e^{-\frac{z}{\gamma_i}}, \quad z \geq 0. \tag{1}$$

We assume that user channels are independently distributed *but not identically*, and the channel state information is available at the base station. Transmissions occur at different rates according to M available modulation and coding schemes (MCSs), selected as a function of the instantaneous SNR, i.e., for user i:

$$MCS_i = k \iff \Gamma_i \in [th_k; th_{k+1}), \; k = 1 \dots M; \tag{2}$$

$$th_1 = 0; th_p < th_q \iff p < q; \quad th_{M+1} = \infty,$$

where the SNR thresholds th_k are expressed in linear units.

Therefore, the probability that a scheduled user i transmits a frame encoded with the kth MCS is:

$$\pi_k^{(i)} = \int_{th_k}^{th_{k+1}} dF_i(z) = e^{\frac{th_k}{\gamma_i}} - e^{\frac{th_{k+1}}{\gamma_i}}. \tag{3}$$

We denote b_k by the number of data bits transferred in one OFDMA symbol using the kth MCS, as reported in Table 1. Index $k = 1$ corresponds to SNR values below the minimum receiver sensitivity, for which no transmission is possible at all. The table shows the list of possible MCSs with their corresponding SNR thresholds for an LTE-like network [18]. The Implementation Margin (IM) in Table 1 is a value that represents the effects of non-ideal receiver. For the sake of tractability, here we assume that mobile users belong to one of three predefined user channel quality classes (referred to as *user qualities*). These user qualities are characterized by different mean SNR values, and correspond to *poor*, *average*, and *good* users. The designated mean SNR values for different classes are chosen in a manner that the mean achievable rates for *poor*, *average*, and *good* users are 20%, 50%, and 80% of the maximum transmission rate achievable in the system, respectively. Considering the thresholds and MCS values reported in Table 1, the designated mean SNR values are 7dB, 16dB and 23dB, respectively for *poor*, *average*, and *good* users. Note that using non-homogeneous channel qualities allows us to evaluate the long-term system fairness under different (opportunistic)

Table 1: Modulation and coding schemes and their thresholds

Modulation	**Coding Rate**	**SNR** (dB)	**IM** (dB)	**SNR+IM** (dB)	b_k (Bits per symbol)
-	-	-∞	-	-∞	$b_1 = 0$
QPSK	1/8	-5.1	2.5	-2.6	$b_2 = 0.25$
	1/5	-2.9		-0.4	$b_3 = 0.4$
	1/4	-1.7		0.8	$b_4 = 0.5$
	1/3	-1		1.5	$b_5 = 0.67$
	1/2	2		4.5	$b_6 = 1$
	2/3	4.3		6.8	$b_7 = 1.3$
	3/4	5.5		8.0	$b_8 = 1.5$
	4/5	6.2		8.7	$b_9 = 1.6$
16QAM	1/2	7.9	3	10.9	$b_{10} = 2$
	2/3	11.3		14.3	$b_{11} = 2.66$
	3/4	12.2		15.2	$b_{12} = 3$
	4/5	12.8		15.8	$b_{13} = 3.2$
64QAM	2/3	15.3	4	19.3	$b_{14} = 4$
	3/4	17.5		21.5	$b_{15} = 4.5$
	4/5	18.6		22.6	$b_{16} = 4.8$

scheduling mechanisms. For simplicity, we report the notation used throughout the manuscript in Table 2.

For the proposed system, the analysis of throughput and power consumption is presented in what follows.

Table 2: Notation used within this manuscript

Notation	Description
N	Total number of users.
M	Number of *MCS*s.
N_c	Number of clusters.
C_n	Set of users in the n^{th} cluster.
N_n	Number of members of cluster C_n.
S_{tot}	Total uplink resources (symbols/frame).
t_k^i	Resources allocated to user i when $MCS_i = k$.
γ_i	Mean SNR of user i.
th_k	Minimum SNR for transmitting with the k^{th} *MCS*.
b_k	Data bits per symbol in the k^{th} *MCS*.
π_k	Probability to transmit with the k^{th} *MCS*.
P_h^i	Probability of user i being cluster head.
P_a	Probability of interface being active.
$W_{(.)}$	Power consumption.
$\beta_{(.)}$	Baseline power of the interface in active mode.
$\beta_{(.)}^{idle}$	Baseline power of the interface in idle (power saving) mode.
$\alpha_{(.)}$	Power consumption per Mbps over LTE.
$\zeta_{(.)}$	Power consumption per Mbps over WiFi.
$\tau_{(.)}$	Fraction of time spent on transmission over WiFi.
$\kappa_{(.)}$	Power consumed due to packet processing over WiFi.
$\lambda_{(.)}$	Packet rate.
L_p	Average packet size.
$R_{tx}^{i,lte}$	Average data rate of user i over LTE.
$R_{tx}^{i,wifi}$	Average transmission data rate of user i over WiFi.
$R_{rx}^{i,wifi}$	Average reception data rate of user i over WiFi.
R_{wifi}	Achievable rate of WiFi connection.
T_i	Throughput of user i.
T_{C_n}	Throughput of cluster n.
δ_i	Fraction of total cluster throughput belonging to user i.
$F_X(.)$	*CDF* of random variable X.

3.2. DRONEE Throughput Modeling

Here we detail two opportunistic cluster head selection and scheduling schemes, and model the throughput attained by mobile users. In particular, we analyze two simple schemes, namely DRONEE-W and DRONEE-M. We focus on *simple* mechanisms since the complexity of *throughput-fair* opportunistic operations represents the most serious obstacle towards the practical adoption of opportunistic mechanisms in real systems [19]. Indeed, without user cooperation, pure opportunistic schedulers can be simple to implement and run, but they would behave unfairly [20].

It is shown that even *very simple opportunistic mechanisms can achieve high energy efficiency when using DRONEE*, without sacrificing throughput fairness. Moreover, our DRONEE proposal reduces the complexity of scheduling in general, since only cluster heads can be scheduled by the base station.

Since the base station only communicates with the cluster head, clusters are treated and scheduled as regular users characterized by the aggregate traffic demand of cluster members. From a modeling perspective, a cluster can be considered as a user whose channel state is the highest of the channel states among cluster members. In DRONEE, we consider the case in which the base station schedules N_c clusters instead of N normal users. This means that the base station decides which clusters have to be served, and then transmissions will be managed by the current cluster head.

Defining X_n as the SNR of cluster n, we have:

$$X_n = \max\{\Gamma_j, j \in C_n\},\ n \in \{1 \dots N_c\}. \tag{4}$$

Considering that the random variables Γ_j are all independent, the CDF of X_n can be computed as follows:

$$F_{X_n}(z) = \prod_{j \in C_n} F_j(z) = \prod_{j \in C_n} \left(1 - e^{-\frac{z}{\gamma_j}}\right),\ z \geq 0. \tag{5}$$

The adopted MCS scheme, for each transmission, only depends on the instantaneous SNR of the best channel in the scheduled cluster, i.e., it only depends on X_n at the scheduling epoch. The probability to transmit with k^{th} MCS is given by:

$$\pi_k^{(C_n)} = \int_{th_k}^{th_{k+1}} dF_{X_n}(z). \tag{6}$$

3.2.1. DRONEE-W

The first proposed scheme schedules clusters in a Weighted Round Robin (WRR) fashion, and selects the cluster head as the user with the strongest channel quality in its cluster. We name this scheme DRONEE-W. The weights w_n associated with each cluster C_n can be assigned in a variety of methods. For simplicity, we will associate weights to clusters based on their size. Thus, denoting N_n as the number of members of cluster C_n, we can compute the weights as $w_n = N_n/N$.

The per-cluster scheduling probability is w_n, $n \in \{1 \dots N_c\}$, while the transmission rate depends on the channel seen by the cluster head, as given by the probability mass function described in (6). Since resources S_{tot} are allocated in WRR style, the average cluster throughput and the average per-user throughput are given by the following Propositions 1 and 2, whose proofs are immediate, so we omit them.

Proposition 1. *Under DRONEE-W, the average throughput received by cluster C_n is*

$$E[T_{C_n}] = w_n S_{tot} \sum_{k=1}^{M} \pi_k^{(C_n)} b_k,\ \ n \in \{1 \dots N_c\}. \tag{7}$$

Proposition 2. *Under DRONEE-W, the average throughput received by user $i \in C_n$ can be expressed as*

$$E[T_i] = \frac{S_{tot}}{N} \sum_{k=1}^{M} \pi_k^{(C_n)} b_k,\ i \in C_n,\ n \in \{1 \dots N_c\}. \tag{8}$$

The probability that a user i is scheduled is given in the following proposition.

Proposition 3. *Under DRONEE-W, a user $i \in C_n$ is scheduled with probability*

$$P_h^{(i)} = w_n \sum_{k=1}^{M} \pi_k^{(C_n)} \int_0^{\infty} [1 - F_i(z|MCS_i = k)]\, dF_{Y_i}(z), \quad (9)$$

where $Y_i = \max_{j \in C_n \setminus \{i\}} \{\Gamma_j\}$, $i \in C_n$.

The proof of Proposition 3 is reported in Appendix A. Note that, under Rayleigh fading assumptions, the conditional probability $F_i(z|MCS_i = k)$ is simply given by the following formula:

$$F_i(z|MCS_i = k) = \frac{F_i(\min(z, th_{k+1})) - F_i(th_k)}{\pi_k^{(i)}},\ z \geq th_k. \quad (10)$$

3.2.2. DRONEE-M

With this second scheme, in each frame, our system selects the cluster which has the user with the best channel quality and assigns all resources S_{tot} to it. That user is selected as cluster head for its cluster. Therefore, DRONEE-M performs the cluster head selection and scheduling according to a pure MaxRate approach [21].

The average cluster throughput and the average per-user throughput achieved under DRONEE-M are given by the following Propositions 4 and 5.

Proposition 4. *Under DRONEE-M, the average throughput received by cluster C_n is*

$$E[T_{C_n}] = S_{tot} \sum_{k=1}^{M} \Big[\pi_k^{(C_n)} b_k \times \int_0^{\infty} [1 - F_{X_n}(z|MCS_{C_n} = k)]\, dF_{Y_n}(z) \Big], \quad (11)$$

where $n \in \{1 \ldots N_c\}$, X_n is defined in (4)*, and $Y_n = \max_{j \notin C_n} \{\Gamma_j\}$.*

The proof of Proposition 4 is reported in Appendix A.

Proposition 5. *Under DRONEE-M, the average throughput received by user $i \in C_n$ is*

$$E[T_i] = \frac{S_{tot}}{N_n} \sum_{k=1}^{M} \Big[\pi_k^{(C_n)} b_k \times \int_0^{\infty} [1 - F_{X_n}(z|MCS_{C_n} = k)]\, dF_{Y_n}(z) \Big], \quad (12)$$

where $n \in \{1 \ldots N_c\}$, X_n is defined in (4)*, and $Y_n = \max_{j \notin C_n} \{\Gamma_j\}$.*

The proof of Proposition 5 is like the proof of Proposition 4.

The probability that a user i is scheduled is given in the following proposition, which is proven in Appendix A.

Proposition 6. *Under DRONEE-M, a user i is scheduled with probability*

$$P_h^{(i)} = \sum_{k=1}^{M} \pi_k^{(i)} \int_0^{\infty} [1 - F_i(z|MCS_i = k)]\, dF_{Y_i}(z), \quad (13)$$

where $Y_i = \max_{j \neq i} \{\Gamma_j\}$ and $F_i(z|MCS_i = k)$ is given by Eq. (10)*.*

3.3. DRONEE Power Consumption

We derive the power consumption of mobiles in DRONEE from the empirical power models proposed for LTE and WiFi in [9] and [10]. Differently from the existing models, our proposed power model distinguishes between the power consumption in active and idle periods, the transmission power, and the reception power. By doing so, our model accounts for the power saving features that LTE and WiFi technologies incorporate, which allows users to switch off part of the circuitry for most of the idle-interval duration.

In what follows, we distinguish between average throughput $E[T]$ and data rate R of a user. The former is the amount of user-application local data received by a user directly via LTE or via WiFi relay, and it is computed via (8) and (12). The latter is the amount of data handled by a user over a wireless interface, and it includes non-local traffic to be relayed.

3.3.1. Power saving in LTE and WiFi

In LTE, idle periods are handled by discontinuous reception *DRX* and discontinuous transmission *DTX* mechanisms [22]. In WiFi, users can turn off the wireless interface during idle periods and only switch it on to receive beacons [23]. In both LTE and WiFi, interfaces in power saving mode periodically wake up to transmit/receive control information even if there is no data traffic to handle. However, it has been shown that the periodic wake-up of power saving mechanisms in LTE and WiFi impacts at most 5% of the idle time [9]. Therefore, for simplicity, we ignore the periodic wake-up operation. We assume that wireless interfaces can instantaneously switch from active to power saving mode as soon as there are no packets to be handled by that interface. Interfaces switch back to active mode as soon as a packet is present in the transmission queue. Therefore, in our model, interfaces stay in power saving mode during the entire idle interval. In light of this assumption, we interchangeably use the expressions *power saving mode* and *idle mode*.

3.3.2. LTE consumption

According to [9], the LTE power consumption results from the sum of a baseline power and a term which is proportional to the transmission rate of the device. Here, we extend the model provided in [9] by considering the probability that user i is in active mode over the LTE interface, which is equivalent to the probability $P_h^{(i)}$ of being the cluster head given in Eqs. (9) and (13). The power spent by user i over LTE can be computed as follows:

$$W_{lte}^{(i)} = P_h^{(i)} \beta_{lte} + \left(1 - P_h^{(i)}\right) \beta_{lte}^{idle} + \alpha_{tx} R_{tx}^{(i,lte)}, \quad (14)$$

where, β_{lte} and β_{lte}^{idle} are the baseline powers in active and idle mode, respectively; α_{tx} is the power consumption per Mbps in uplink, and $R_{tx}^{(i,lte)}$ is the average data rate transmitted by user i over the LTE interface. The value of $R_{tx}^{(i,lte)}$ is computed using the following two propositions.

Proposition 7. *Using DRONEE-W, the uplink LTE data rate of user $i \in C_n$ is given by*

$$R_{tx}^{(i,lte)} = w_n S_{tot} \sum_{k=1}^{M} \pi_k^{(C_n)} b_k \int_0^{\infty} [1 - F_i(z|MCS_i = k)]\, dF_{Y_i}(z); \tag{15}$$

where $Y_i = \max_{j \in C_n \setminus \{i\}} \{\Gamma_j\}$, $i \in C_n$.

The proof of Proposition 7 is omitted since it follows the same scheme of the proof of Proposition 3, considering that, with DRONEE-W, in the kth MCS the achieved data rate is $w_n S_{tot} b_k$.

Proposition 8. *Using DRONEE-M, the uplink LTE data rate of user $i \in C_n$ is given by*

$$R_{tx}^{(i,lte)} = S_{tot} \sum_{k=1}^{M} \pi_k^{(i)} b_k \int_0^{\infty} [1 - F_i(z|MCS_i = k)]\, dF_{Y_i}(z); \tag{16}$$

where $Y_i = \max_{j \neq i} \{\Gamma_j\}$, $i \in C_n$.

The proof of Proposition 8 is omitted since it follows the same scheme of the proof of Proposition 6, considering that, with DRONEE-M, in the kth MCS the achieved data rate is $S_{tot} b_k$.

3.3.3. WiFi consumption

As for WiFi consumption, we enhance the model proposed in [10], which accounts for the power required for packet processing as well as for transmission. We additionally add the probability that the WiFi interface of user i is in active mode $P_a^{(i)}$. The resulting WiFi power consumption can be expressed as follows:

$$\begin{aligned} W_{wifi}^{(i)} = {} & P_a^{(i)} \beta_{wifi} + \left(1 - P_a^{(i)}\right) \beta_{wifi}^{idle} \\ & + \zeta_{tx}\tau_{tx} + \zeta_{rx}\tau_{rx} + \kappa_{tx}\lambda_{tx} + \kappa_{rx}\lambda_{rx}, \end{aligned} \tag{17}$$

where β_{wifi} and β_{wifi}^{idle} are the WiFi baseline powers in active and idle mode, respectively; ζ_{tx} and ζ_{rx} represent the power consumptions due to transmission and reception, respectively; τ_{tx} and τ_{rx} are the fractions of time spent in transmission and reception, respectively; κ_{tx} and κ_{rx} are the power consumptions due to packet processing in transmission and reception, respectively; eventually, λ_{tx} and λ_{rx} are the packet rates, respectively in transmission and reception.

The WiFi power consumption related parameters introduced in Eq. (17) are computed as follows: (*i*) τ_{rx} is the ratio between the transmission rate over the WiFi interface and the achievable rate of the WiFi connection, i.e., for user i, we have $\tau_{rx}^{(i)} = R_{rx}^{(i,wifi)}/R_{wifi}$; (*ii*) similarly, $\tau_{tx}^{(i)}$ is given by $R_{tx}^{(i,wifi)}/R_{wifi}$; (*iii*) user i receives $\lambda_{rx}^{(i,wifi)}$ packets per second over the WiFi interface, which can be computed as the ratio between the rate $R_{rx}^{(i,wifi)}$ and the average packet size L_p; and (*iv*) similarly, user i transmits $\lambda_{tx}^{(i,wifi)} = R_{tx}^{(i,wifi)}/L_p$ packets per second. We assume that the achievable WiFi rate in each cluster is independent from the cellular network status and its average value R_{wifi} is the same for all clusters (i.e., this is an input parameter for our problem). If the achievable WiFi rate is larger than the intra-cluster traffic (i.e., $R_{wifi} > \sum_{i \in C_n} R_{rx}^{(i,wifi)} = \sum_{i \in C_n} R_{tx}^{(i,wifi)}$), then to evaluate the WiFi power consumption, we need to compute the WiFi data rates $R_{rx}^{(i,wifi)}$ and $R_{tx}^{(i,wifi)}$, and the probability $P_a^{(i)}$ that the WiFi interface of user i be active.

The following proposition tells how to compute $R_{rx}^{(i,wifi)}$ and $R_{tx}^{(i,wifi)}$.

Proposition 9. *The WiFi data rate of user $i \in C_n$ is given by the following expressions, which hold for the received and transmitted traffic, respectively:*

$$R_{rx}^{(i,wifi)} = (1 - \delta_i) \cdot R_{tx}^{(i,lte)}, \tag{18}$$

$$R_{tx}^{(i,wifi)} = \delta_i \cdot \sum_{j \in C_n \setminus \{i\}} R_{tx}^{(j,lte)}, \tag{19}$$

where

$$\delta_i = \frac{E[T_i]}{E[T_{C_n}]}. \tag{20}$$

The proof of Proposition 9 is given in Appendix A.

For the probability $P_a^{(i)}$ that the WiFi interface of user i be in active mode, we use the following result:

Proposition 10. *The WiFi interface of user i is active with probability $P_a^{(i)}$ that is computed as follows:*

$$P_a^{(i)} = \frac{E[T_i] + (1 - 2\delta_i) R_{tx}^{(i,lte)}}{R_{wifi}}, \tag{21}$$

with δ_i defined in (20)*.*

The proof of Proposition 10 is reported in Appendix A.

3.3.4. Total consumption

Using the results of Sections 3.3.2 and 3.3.3, the total power consumption due to LTE and WiFi for a clustered user is expressed as follows:

$$\begin{aligned} W_{tot}^{(i)} = {} & \beta_{lte}^{idle} + \beta_{wifi}^{idle} \\ & + \left(\beta_{lte} - \beta_{lte}^{idle}\right) P_h^{(i)} \\ & + \left(\beta_{wifi} - \beta_{wifi}^{idle}\right) \frac{E[T_i] + (1 - 2\delta_i) R_{tx}^{(i,lte)}}{R_{wifi}} \\ & + \alpha_{tx} R_{tx}^{(i,lte)} \\ & + \left(\zeta_{rx} + \frac{\kappa_{rx}}{L_p}\right)(1 - \delta_i) \frac{R_{tx}^{(i,lte)}}{R_{wifi}} \\ & + \left(\zeta_{tx} + \frac{\kappa_{tx}}{L_p}\right) \frac{E[T_i] - \delta_i R_{tx}^{(i,lte)}}{R_{wifi}}. \end{aligned} \tag{22}$$

The first term in Eq. (22) represents the baseline power consumption due to the presence of the two wireless interfaces; the second and third terms are due to increased baseline power consumption, respectively on LTE and WiFi interfaces, when the interfaces are active rather than idle; the forth term accounts for LTE uplink transmissions, while the fifth term is due to the reception of packets over the WiFi interface when the user is cluster head; finally, the last term in Eq. (22) represents the power spent to send WiFi traffic to the cluster head.

4. Numerical Evaluation

In this section we use the model presented in Section 3 to numerically simulate networks with single and multiple base stations. We use LTE uplink frame parameters for a network operating on a 20 MHz bandwidth in FDD mode [17]. Each scenario is simulated 5000 times and the user channel quality changes at random in each simulation (according to a probability distribution that will be specified for each described experiment). Final results are expressed using averages, 25^{th} and 75^{th} percentiles computed over the simulated runs.

The performance of DRONEE-W and DRONEE-M is benchmarked against Round Robin (RR) and proportional fair (PF) schedulers. The implementation details of these schedulers in our simulations can be found in Appendix B. RR and PF do not use clustering, and thus they can be used to compute per-user throughputs only. However, for comparison reasons, for each cluster formed under DRONEE operations, we will present the sum of RR or PF throughputs that cluster members would achieve if DRONEE were not used. Such an aggregate throughput is referred to as the per-cluster RR or PF throughput. To obtain the power consumption of legacy schedulers, we use Eq. (14), in which we replace $P_h^{(i)}$ with the probability of user i being scheduled under RR or PF, respectively.

For our computations, we use an average packet size L_p = 1000 B and average WiFi net rate R_{wifi} = 30 Mbps, which is a reasonable net data rate achievable for 802.11a/g standards [24]. The values for power related parameters used in the evaluation can be found in Table 3 and are derived from [9, 10].

Table 3: Parameters used in the power model

LTE			WiFi					
β_{lte}	β_{lte}^{idle}	α_{tx}	β_{wifi}	β_{wifi}^{idle}	ζ_{tx}	ζ_{rx}	κ_{tx}	κ_{rx}
1.29 [W]	0.59 [W]	438.39 [nW/bps]	0.14 [W]	0.08 [W]	0.46 [W]	0.44 [W]	0.11 [mJ]	0.09 [mJ]

4.1. Clustering Impact

Before evaluating DRONEE, let us first evaluate the fundamental factors that can affect its performance: (*i*) the channel quality of the cluster members (see Figure 2(a)); and (*ii*) the cluster size (see Figure 2(b)). The importance of the former factor can be observed by comparing the user's channel state probabilities, as defined in Eq. (3). The primary effect of opportunistic cluster head selection is to increase the probability of transmitting with higher MCS values. This effect magnifies in clusters with *poor* and *good* users where the *good* users help the *poor* ones and increase the probability of transmission with a high MCS. In Figure 2(a), we observe that, with a cluster composed of one user from each quality class (C1 in the figure), the transmission rate of *poor* and *average* users highly boosts. Since transmission probabilities for *poor* and *average* users are mostly accumulated in low transmission rates, the clustering improvement for *good* users is marginal. We note that increasing the cluster size significantly increases the probability of using high transmission rates (see case C2 in the figure).

Figure 2(b) illustrates the achieved spectral efficiency for different cluster sizes. Here we use the spectral efficiency instead of the achieved throughput so that the results are independent on the airtime allocated to the cluster in the presence of other

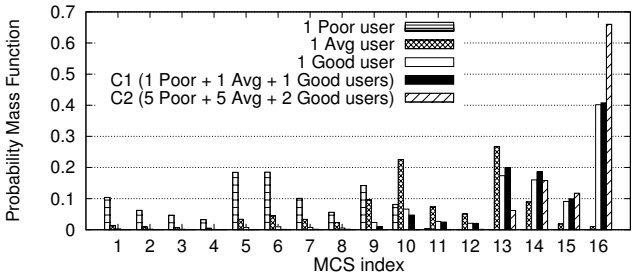

(a) Impact of clustering on channel state probabilities.

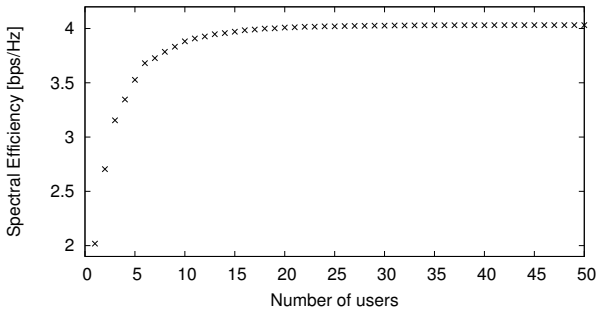

(b) Impact of cluster size on spectral efficiency of the cluster.

Figure 2: Impact of clustering on channel state probabilities and spectral efficiency.

clusters. Since each addition of an extra cluster member increases the probability of transmitting with higher MCSs, it is natural to expect that this probability will eventually approach to one. In Figure 2(b), such saturation occurs after the cluster size reaches 6 users with uniform random user quality distribution. As the cluster size increases from 7 to 50 users, the spectral efficiency experiences a *saturation effect*, which consists in marginally small successive improvements. Therefore, forming very large clusters is not beneficial in terms of spectral efficiency.

4.2. Clustering in a Single Cell Network

We begin the evaluation of energy efficiency and resource utilization with a simple scenario comprising three fixed-size clusters, which are attached to the same eNB, as shown in Figure 3. Clusters have different sizes and cluster members have independent but not identically distributed SNRs. Unless otherwise specified, user qualities are chosen according to a uniform random distribution. Figure 4 illustrates the throughput performance of different scheduling algorithms.

In Figure 4(a), it can be observed that the average per-user throughput is substantially higher under DRONEE variants than

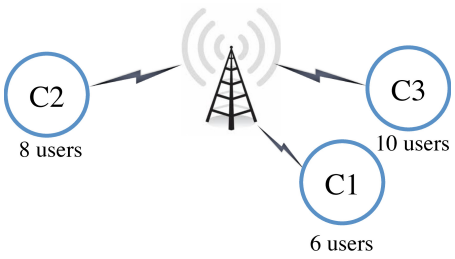

Figure 3: Evaluation topology for static clusters.

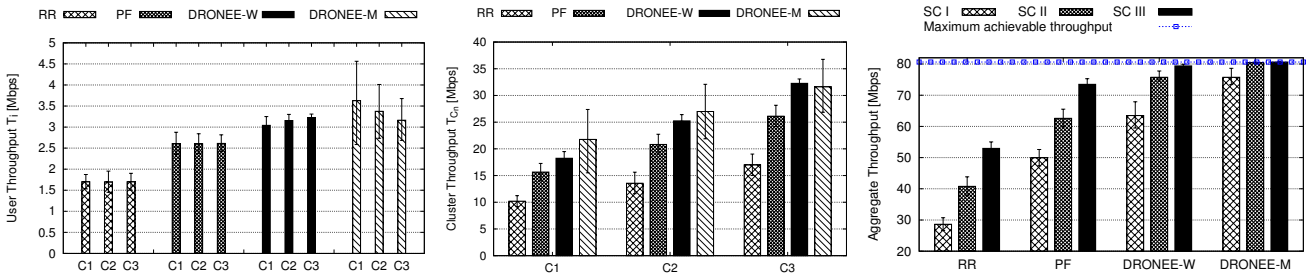

(a) Per-user per-cluster throughput. (b) Aggregate per-cluster throughput. (c) Aggregate cell throughput.

Figure 4: Per-user, per-cluster, and aggregate throughput for single cell scenario (Figure 3).

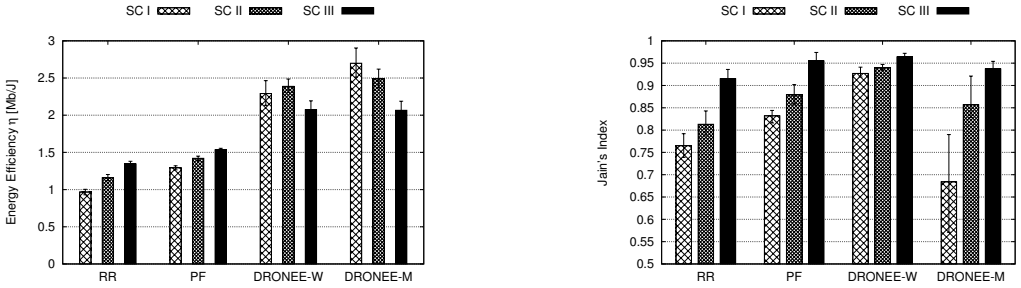

(a) Per-user energy efficiency. (b) Per-user Jain's fairness indexes.

Figure 5: Energy efficiency and fairness performance under different user quality distributions.

under legacy schedulers. DRONEE outperforms RR and PF due to its more efficient use of spectrum, which is the result of opportunistic selection of cluster heads (cooperative gain). Since the cluster head is the user with the highest instantaneous channel quality, the cluster resource utilization is maximized at each scheduling epoch. The high variation observed under DRONEE-M is due to its greedy behavior that can lead to starvation of clusters with only *poor* and *average* users and overserving the clusters with *good* users. RR performs the worst because it schedules the users regardless of their channel quality. In contrast, PF uses an opportunistic scheduling technique that results in remarkable throughput enhancement in comparison to RR. Nevertheless, DRONEE-M and DRONEE-W largely outperform PF.

Figure 4(b) shows that all clusters receive higher throughput with DRONEE than with legacy schedulers. Bigger clusters receive more airtime under RR, PF, and DRONEE-W because the airtime allotted to clusters is *deterministic* and proportional to the number of cluster members. Under DRONEE-M the airtime grows *statistically* with the cluster size because adding an extra member increases the probability of having the user which has the best MCS in the cell. Therefore, with a pure MaxRate approach, such as in DRONEE-M, cluster throughputs will suffer from the saturation effect discussed earlier and depicted in Figure 2(b). In contrast, distributing resources proportional to cluster sizes, as in DRONEE-W, delays the occurrence of saturation. This effect can be observed in Figure 4(b): as the cluster size increases from 6 in C1 to 10 in C3, throughputs grow faster with DRONEE-W than with DRONEE-M.

Figure 4(c) illustrates aggregate cell throughputs under different user quality distributions. In order to evaluate the impact of user quality distribution on the performance of our proposal, we consider three scenario sub-cases, characterized by different user quality distributions as stated in Table 4.

The results shown in Figure 4(c) confirm that DRONEE has higher throughput than user-based schedulers regardless of user quality distributions. DRONEE-M has better throughput performance than DRONEE-W because it always schedules the cluster head with the best channel quality (opportunistic gain). In contrast, DRONEE-W distributes the resources among clusters based on their size and not the channel quality of cluster heads. Nevertheless, the throughput gains are affected by user quality distribution. The throughput gain of DRONEE over RR increases from 50% to 162% as we move from sub-case SC III to SC II and SC I, i.e., as the percentage of *good* users reduces. Similarly, the gain over PF ranges approximately from 12% to 50% over the different sub-cases. The increment in throughput gain is due to the fact that increasing the number of *poor* users, also increases the opportunity for DRONEE to enhance the spectral efficiency of the system. The throughput gain of DRONEE over PF is less than that of RR due to the opportunistic nature of the PF scheduler. Figure 4(c) also shows that the system has near optimal performance with DRONEE when as few as 33% of the users are *good* (sub-case SC II).

Figure 5(a) confirms the energy efficiency significance of our proposal. It can be seen that DRONEE variants are much

Table 4: User quality distributions used in different scenarios

Scenario sub-case	% of poor users	% of avg users	% of good users
SC I	60%	30%	10%
SC II	$33.\overline{3}$%	$33.\overline{3}$%	$33.\overline{3}$%
SC III	10%	30%	60%

more energy efficient than legacy mechanisms. Indeed, using DRONEE provides a minimum gain of 30% in energy efficiency with respect to PF (sub-case SC III), and the gain can reach up to 100% in the presence of more *poor* users (sub-case SC I). The energy efficiency gain with respect to RR is even more significant in all sub-cases depicted in Figure 5(a). Therefore, DRONEE not only highly increases the system throughput, but also the cost (energy per bit) of transmission is reduced considerably.

Eventually, we comment about fairness, using the well known Jain's index [25]. Figure 5(b) shows that fairness is the lowest when there are more *poor* users in the system (sub-case SC III). DRONEE-W achieves the highest per-user fairness level in the system, even higher than PF, which is a scheduler designed for fairness. In general, DRONEE has an extra fairness advantage because it allows to distribute the throughput gain achieved via clustering among all cluster members, which leads to smoothening the throughput difference among *poor* and *good* users within the same cluster. However, DRONEE-M still has the worst fairness which is due to its bias towards serving the cluster with the best user in the network, which exceeds the smoothening effect of clustering.

We can summarize the performance results reported in this scenario as follows: (*i*) DRONEE is significantly more energy efficient than RR and PF (up to 100% efficiency gain over PF); (*ii*) DRONEE provides a high throughput gain with respect to legacy RR and PF schedulers (up to 50% throughput gain over PF and 162% over RR); (*iii*) between DRONEE variants, DRONEE-M shows poor fairness in presence of more *poor* users, whilst DRONEE-W outperforms PF and RR in terms of fairness and nearly achieves perfect fairness.

4.3. Clustering Across Cells

Another interesting scenario in which clustering can be beneficial to uplink efficiency is the case of clusters formed by users associated to different eNBs. This scenario is of paramount importance for users located at the edge of their cells, whose channel can suffer from deep fading fluctuations. Clustering is in particular advantageous here because it improves the spectral efficiency of the users with poor channel quality [21].

We evaluate a scenario with three neighboring cells as depicted in Figure 6. In the figure, clusters C3, C4, and C7 result from the merging of two sub-clusters (namely, C*i*a and C*i*b, $i \in \{3, 4, 7\}$) formed by users at the edge of the cells. Each sub-cluster is connected to its corresponding eNB (e.g., C3*a* and C4a are connected to eNB1). Although sub-clusters are connected to different eNBs, they share their resources within the entire cluster via WiFi connectivity. Note that in this scenario, clusters composed of sub-clusters have a different cluster head for each cell in which they have members. Since each user can access two cluster heads in two different cells, they can distribute their load between cells.

In this set of simulations, clusters that are not located at the cell edge have uniform user quality distribution. In contrast, clusters at the edge of cell can have *poor*, *average* and *good* users with probability 60%, 30%, 10%, respectively. In each

Cluster	# of users
C1	[1 , 20]
C2	[1 , 20]
C3a	[1 , 10]
C4a	[1 , 10]
C5	[1 , 15]
C6	[1 , 15]
C4b	[1 , 10]
C7a	[1 , 10]
C8	[1 , 10]
C9	[1 , 10]
C3b	[1 , 5]
C7b	[1 , 5]

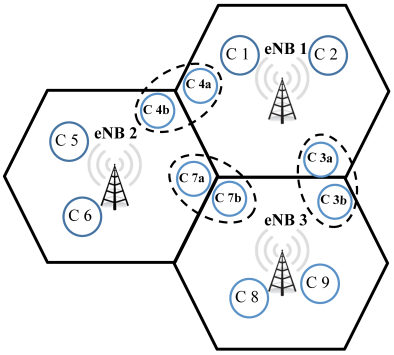

Figure 6: Three base stations with nine clusters. Clusters C3, C4, C7 are composed of two sub-clusters belonging to two adjacent cells.

experiment, cluster sizes change randomly with a uniform distribution, using the ranges reported in Figure 6. These intervals are chosen so that eNB1 has more users than eNB2, and eNB3 has the fewest users, on average. With the multi-cell scenario we add to our performance evaluation the study of the impact of heterogeneity in the geographical distribution of mobile users.

Figure 7 illustrates that DRONEE achieves better throughput performance than legacy schedulers in the multi-cell scenario, under all combinations of cluster sizes and locations. DRONEE-W outperforms PF and RR in terms of per-user and per-cluster throughput in all clusters, see Figures 7(a) and 7(b). In contrast, under DRONEE-M, users located in cell edge clusters (C3, C4, and C7) achieve slightly less throughput than DRONEE-W (~ 0.3 Mbps less); at the same time, users in the other clusters experience better throughput than DRONEE-W (up to ~ 1.8 Mbps more). This happens because DRONEE-M prioritizes the clusters with the best channel quality, so that cell edge clusters have less chance to be scheduled. We can observe in Figure 7(c) that per-cell throughput gain is substantial with DRONEE. Indeed DRONEE-M almost achieves the maximum throughput. Although DRONEE-W achieves less throughput than DRONEE-M, it still brings a considerable throughput gain ($\sim$20%) with respect to PF. Therefore, the results confirm that our proposal achieves higher resource utilization even under the heterogeneous distribution of user locations and with heterogeneous cluster compositions. Moreover, our results point out that cluster size matters, as witnessed by the fact that users under eNB3 achieves lower throughputs than users in other cells. In fact, eNB3 has the smallest user population among the three cells, which leads to smaller cooperative gain (see Figure 2(b)).

Figure 8(a) shows that our proposal highly improves energy efficiency of users (54% to 77% with respect to PF). DRONEE has better energy efficiency because it reduces the energy per bit transmission cost by increasing the spectral efficiency of the network. In general, we observe that with fewer users we can achieve higher energy efficiency under all scheduling disciplines (the efficiency in eNB3 is always the highest, with or without clusters). This can be explained by looking into the definition of energy efficiency, which is given by *per-user throughput over power consumption*. Now, while increasing the number of users significantly reduces the per-user throughput, the per-user power consumption—which is mainly due to the baseline power required by the wireless interfaces—suffers lit-

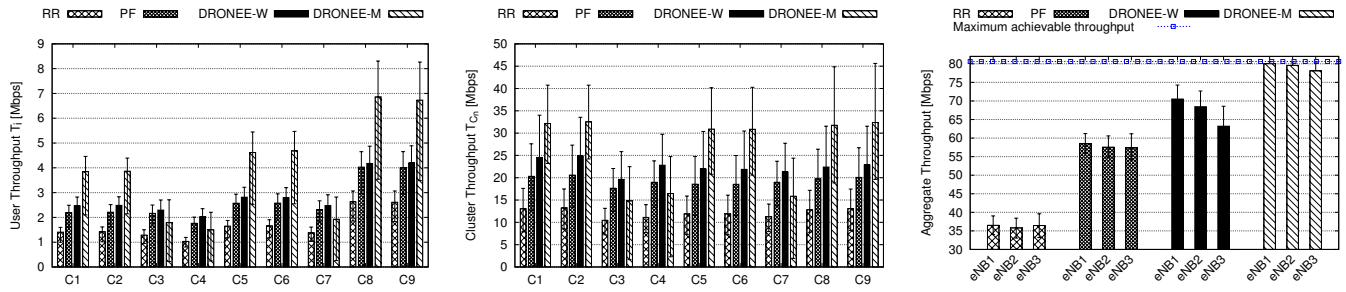

(a) Per-user throughput. (b) Per-cluster throughput. (c) Aggregate throughput per cell.

Figure 7: Throughput under different scheduling mechanisms for the multi-cell scenario.

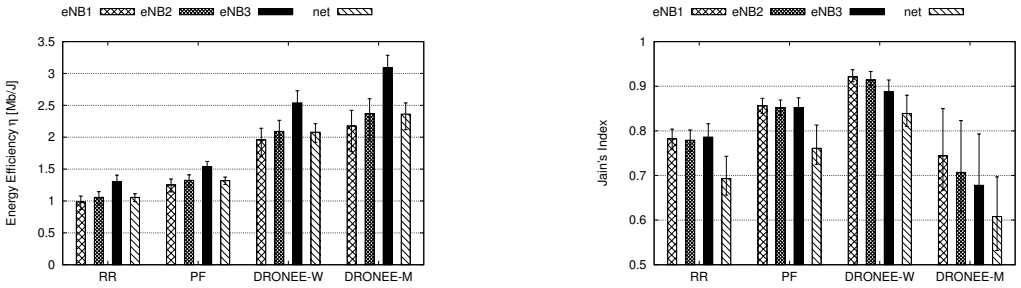

(a) Per-cell energy efficiency. (b) Per-user Jain's fairness indexes.

Figure 8: Energy efficiency and per-user fairness under different scheduling mechanisms for the multi-cell scenario. The *net* values reported in the figures represent the average performance observed over the three-cell network of Figure 6.

tle variations. Therefore, *large cell populations are inherently energy inefficient*, which makes it of paramount importance to boost the energy efficiency of dense networks. Notably, our proposal introduces such a significant leap in efficiency. Moreover, according to our results, clustering boosts energy efficiency, but large clusters are not needed to achieve high energy efficiency.

Eventually, Figure 8(b) illustrates the fairness achieved in each cell. DRONEE-W provides the highest fairness in the system. As discussed earlier, DRONEE-M prioritizes the clusters with high channel quality over cell edge clusters, which results in big throughput differences among users and poor fairness performance in the multi-cell scenario. Cells with lower user population are generally prone to lower user fairness due to the compound effect of the following factors: (*i*) per-user allocated airtime is larger in small cells; (*ii*) *good* users can exploit the extra airtime obtained thanks to clustering better than *poor* users; and (*iii*) the advantage deriving from the presence of *good* users in a cluster is not shared among clusters. As a result, the throughput difference among users in small and heterogeneous cells is higher and results in lower fairness indexes if compared to the results for larger cells.

Summarizing the results discussed in this sub-section, we conclude that: (*i*) DRONEE highly improves the energy efficiency with respect to RR and PF, which is particularly useful in case of dense networks, where the efficiency is impaired by the baseline consumption of (idle) users; (*ii*) DRONEE provides a high throughput gain with respect to legacy RR and PF schedulers, irrespective of the cell size; (*iii*) between DRONEE variants, DRONEE-M shows poor fairness performance due to its bias towards serving *good* users; whilst (*iv*) DRONEE-W outperforms PF and RR and achieves the highest fairness levels in a variety of scenarios, i.e., under different distributions of users over cells and clusters.

5. DRONEE Implementability over LTE and WiFi Direct

In this section, we corroborate the practical relevance of DRONEE by providing a first-order discussion on its implementability. We use LTE release 10 [17] and WiFi Direct [26] specifications to show that our proposal can be implemented on top of existing and widespread technologies.

The key procedures composing the protocol needed to implement opportunistic clustering using LTE and WiFi Direct are the following: (*i*) *cluster formation*, which allows mobile devices to find and join existing clusters or setup new clusters using the WiFi interface; (*ii*) *registration*, to make the LTE eNB aware of the cluster existence and composition; (*iii*) *grant request*, to allow the cluster head to request a cumulative traffic grant which covers the demand of the entire cluster; (*iv*) *Channel State Information (CSI) collection*, to collect channel state information at the LTE eNB; (*v*) *cluster head selection*, to decide which user behaves as cluster head, based on the collected channel state information; (*vi*) *bearer allocation*, to allocate portions of the uplink frame to cluster heads instead of any cluster members; (*vii*) *scheduling*, to allocate resources among clusters (scheduling of clusters as if they were users); (*viii*) *resource sharing*, to share resources among cluster members, using WiFi Direct (intra-cluster resource sharing procedure); and (*ix*) *security*, to protect relayed traffic.

Before presenting the network procedures needed to implement DRONEE, it is crucial to recall how LTE handles user communications. In LTE, mobiles are connected to the network via *bearers*. A bearer is a data pipe that is used for data transfer between the user and the network. Each bearer has a specific Quality of Service (QoS) that depends on the type of the traffic carried over the bearer [27]. For example, a VoIP connection and an HTML connection from the same device are established on separate bearers.

Cluster formation. The cluster formation can be easily performed using WiFi Direct group formation capabilities. The mobile device willing to form a cluster can transmit a *Probe Request* on WiFi *Social Channels*, i.e., channels 1, 6 and 11 in the 2.4 GHz ISM band. Alternatively, the device can listen to Probe Requests on Social Channels in order to join existing clusters or other devices willing to form a cluster. WiFi Direct specifications state that the group formation shall not take more than fifteen seconds. Moreover, cluster members meeting each other on a regular basis, can use *persistent groups* as defined in the standard to reduce the cluster formation time. Given the current group formation speed of WiFi Direct, our proposal is attractive in scenarios in which the expected cluster life is in order of minutes. For instance, the cluster formation overhead is negligible for users sharing significant time in the public transportation system or during dense public events such as football matches or concerts, in which users usually experience low quality service due to overloaded infrastructure.

Registration. Once a cluster is formed, the cluster head sends a *cluster formation notification message* to the eNB over the *common/dedicated control channel*, which is used for RRC connection establishment. Next, the eNB forwards the notification message, which contains the identities of cluster members, to the Policy and Charging Enforcement Function (PCEF). Finally, the PCEF checks the status of the current bearers associated to the cluster members and allocates *new cluster specific bearer(s)* accordingly. Depending on the number and the type of applications used in the cluster, a cluster can be allocated one or more bearers. When a member joins or leaves the cluster, the current cluster head can use the Physical Uplink Control CHannel (PUCCH) to send a notification to PCEF to update the cluster membership list and the QoS profile of the bearer(s) allocated to the cluster.

Grant request. LTE devices in a cluster, but the cluster head, prepare their grant requests for uplink traffic and forward it to the cluster head, encapsulating the request in a normal WiFi packet. Then the cluster head sends a single LTE uplink traffic grant request for the bearer associated to the cluster head. Alternatively the cluster head can just forward all traffic grant requests to the eNB, which will map all traffic grant requests to the special cluster bearer(s). In any case, the eNB is not responsible for the repartition of resources within the cluster. Note that using special cluster bearers at the eNB dramatically simplifies the scheduling operation of the base station.

CSI collection. Since mobile devices in LTE regularly perform channel quality measurements, they can inform the cluster head regarding their channel state information by sending the CSI using WiFi Direct. The cluster head collects the channel state information for the entire cluster, but it sends to the eNB only the channel state information for the node who will be the next cluster head (see below for the detail on the procedure to select the cluster head).

Cluster head selection. The cluster head selection procedure is performed locally in each cluster, without imposing extra burden on the eNB. The cluster head collects LTE channel state information from the other cluster members, and decides whether in the next cluster scheduling interval it should keep the role of cluster head or select a new cluster head. The cluster head is responsible to broadcast a WiFi message regarding the identity of the next cluster head to all cluster members. Moreover, it has to notify the eNB about the change of cluster head. The message sent to the eNB to notify it of the identity of the next cluster head also contains the channel state information of the next cluster head. This is beneficial for LTE capacity, because it eliminates the need to allocate bandwidth for feedback from other cluster members. Note that WiFi Direct does not allow cluster members to transfer the group ownership among themselves, however, it is possible to have parallel overlay groups, each with a different group owner. Thus, every cluster member can create a group where it is the group owner and the rest of the cluster members are WiFi Direct *clients*. In every frame, the group owner which is also the cluster head controls the channel. Since the rest of the cluster members are notified about the next cluster head, there will be no interference and collisions among overlay groups. According to the results presented in Section 4, forming clusters with more than ten members has marginal benefits in terms of efficiency; hence, the number of needed overlay WiFi Direct groups is practically limited to a few units.

Bearer allocation. Once the cluster is registered at the eNB, all LTE traffic bearers associated to any cluster member are mapped onto the special cluster bearer(s). This way, the eNB frame builder can allocate uplink resources to the cluster bearer(s) by using the channel state information of the cluster head at any scheduling epoch.

Scheduling. In the presence of multiple clusters, the amount of resources allocated to each cluster head is decided based on DRONEE-M or DRONEE-W. This procedure requires the knowledge of the CSI of the cluster heads, and, in the case of DRONEE-W, the number of cluster members in each cluster. This information is available at the eNB, thanks to the above described procedures used to collect channel state information and to register clusters (and cluster members) at the eNB.

Resource sharing. Figure 9 represents the data plane of the protocol stack used in DRONEE. As depicted in the figure, the cluster head keeps a queue Q_i for each cluster member i, to separately store the traffic received over the WiFi interface, plus a queue for its own uplink traffic. As described above, the resource distribution among clusters is handled by the eNB as if clusters were normal users. The eNB uses the Physical Downlink Control CHannel (PDCCH) to inform the cluster head about the granted resources and their owners. Alternatively, the cluster head can receive a cumulative grant and locally distribute the resources among the uplink queues using simple policies, e.g., equal time, equal rate, etc.

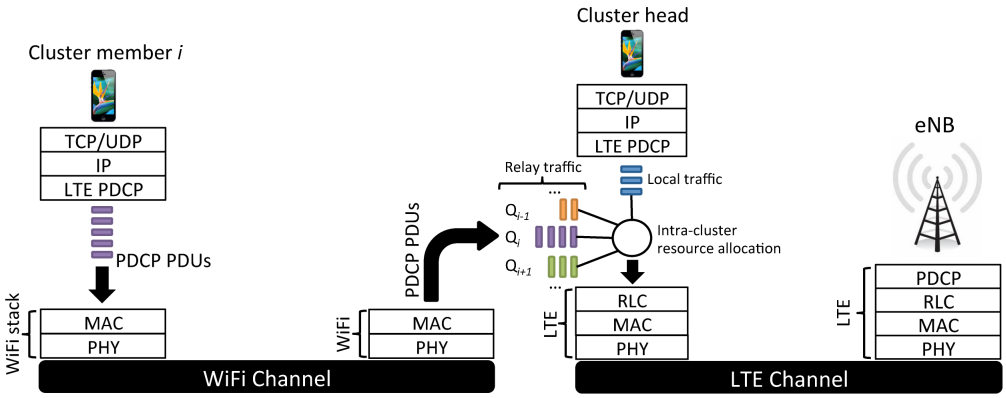

Figure 9: Data flow for uplink traffic generated at the cluster head and at other cluster members in a cellular network using DRONEE.

Security. DRONEE requires cluster members to cipher their traffic according to LTE specifications. In LTE, ciphering is done in the Packet Data Convergence Protocol (PDCP) layer before the Radio Link Control (RLC) and MAC layers. As shown in Figure 9, we extend the ciphering requirement to the traffic that has to be relayed, although that traffic has to go through the WiFi protocol stack. Therefore, in DRONEE, cluster members use ciphered PDCP PDUs as payload of the WiFi frames that have to be sent to the cluster head for relay. Although the cluster head cannot read the ciphered data, it can process and forward each PDCP PDU through RLC, MAC and PHY layers, thus relaying it to the eNB. However, the relayed traffic has to carry the MAC identifier of the original sender, so that the eNB can identify the source of the data and thus decipher it with the correct key. Since the deciphering key is only known to the eNB, the integrity of the relayed traffic will be protected and any data manipulation can be detected by the eNB. Note that, with the described procedure, all PDUs are transmitted exactly as in a legacy LTE system, with no extra protocol overhead being caused by DRONEE. Thanks to this mechanism, DRONEE does not introduce any new security risks to the current LTE architecture.

6. Conclusions

In this article, we have proposed a new approach to seamlessly interwork LTE and WiFi in hybrid networks. Our approach brings significant improvement not only in terms of energy efficiency, but also in terms of throughput and fairness. We have also shown that our proposal could be implemented in a real system using LTE and WiFi technologies. It is shown that our proposal is effective in several scenarios, spanning from single cell scenarios to multiple cells, with variable cell populations and with variable and heterogeneous distributions of user qualities. In particular, DRONEE-W has very desirable properties compared to other schemes. DRONEE-W is simple and scales with network size because it builds on a simple weighted round robin scheduler. It achieves throughputs close to the ones achieved by the throughput optimal scheduler, e.g., MaxRate, and largely outperforms other mechanisms in terms of energy efficiency and achieved fairness. Moreover, our proposed schemes reduce the complexity of scheduling operations, and help both operators—by increasing resource utilization efficiency—and mobile users—by increasing throughput and battery life of their smartphones. Therefore, DRONEE is key to design future energy efficient wireless networks.

7. Acknowledgements

The research leading to these results has received funding from the European Union's Seventh Framework Programme (FP7/2007-2013) under grant agreement n° 318115 (CROWD). This publication was supported in part by the Comunidad de Madrid MEDIANET Project, Ref.: S2009/TIC-1468.

References

[1] N. Balasubramanian, A. Balasubramanian, A. Venkataramani, Energy consumption in mobile phones: a measurement study and implications for network applications, in: Proceedings of ACM IMC, 2009, pp. 280–293.

[2] H. Liu, Y. Zhang, Y. Zhou, Tailtheft: leveraging the wasted time for saving energy in cellular communications, in: Proceedings of ACM MobiArch 2011, ACM, 2011, pp. 31–36.

[3] S. Deng, H. Balakrishnan, Traffic-aware techniques to reduce 3G/LTE wireless energy consumption, in: Proceedings of ACM CoNEXT, 2012, pp. 181–192.

[4] K. Lee, J. Lee, Y. Yi, I. Rhee, S. Chong, Mobile data offloading: how much can WiFi deliver?, in: Proceedings of ACM CoNEXT, 2010, p. 26.

[5] N. Ristanovic, J. Le Boudec, A. Chaintreau, V. Erramilli, Energy efficient offloading of 3G networks, in: Proceedings of IEEE MASS, 2011, pp. 202–211.

[6] L. Lei, Z. Zhong, C. Lin, X. Shen, Operator controlled device-to-device communications in LTE-advanced networks, IEEE Wireless Communications 19 (3) (2012) 96–104.

[7] T. Melia, C. J. Bernardos, A. De La Oliva, F. Giust, M. Calderón, IP flow mobility in PMIPv6 based networks: Solution design and experimental evaluation, Wireless Personal Communications 61 (4) (2011) 603–627.

[8] V. Mancuso, S. Alouf, Analysis of power saving with continuous connectivity, Computer Networks 56 (2012) 2481–2493.

[9] J. Huang, F. Qian, A. Gerber, Z. Mao, S. Sen, O. Spatscheck, A close examination of performance and power characteristics of 4G LTE networks, in: Proceedings of ACM MobiSys, 2012, pp. 225–238.

[10] A. Garcia-Saavedra, P. Serrano, A. Banchs, G. Bianchi, Energy consumption anatomy of 802.11 devices and its implication on modeling and design, in: Proceedings of ACM CoNEXT, New York, NY, USA, 2012, pp. 169–180.

[11] A. Sendonaris, E. Erkip, B. Aazhang, User cooperation diversity. Part I. System description, IEEE Transactions on Communications 51 (11) (2003) 1927–1938.

[12] M. Dohler, et al., Virtual antenna arrays, Ph.D. thesis, University of London (2004).

[13] C.-H. Yu, K. Doppler, C. B. Ribeiro, O. Tirkkonen, Resource sharing optimization for device-to-device communication underlaying cellular networks, IEEE Transactions on Wireless Communications 10 (8) (2011) 2752–2763.

[14] K. Akkarajitsakul, E. Hossain, D. Niyato, Cooperative packet delivery in hybrid wireless mobile networks: A coalitional game approach, IEEE Transactions on Mobile Computing 12 (5) (2013) 840–854.
[15] H. Su, X. Zhang, Clustering-based multichannel MAC protocols for QoS provisionings over vehicular ad hoc networks, IEEE Transactions on Vehicular Technology 56 (6) (2007) 3309–3323.
[16] S. Bandyopadhyay, E. J. Coyle, An energy efficient hierarchical clustering algorithm for wireless sensor networks, in: Proceedings of IEEE INFOCOM, Vol. 3, IEEE, 2003, pp. 1713–1723.
[17] Third Generation Partnership Project (3GPP), Physical layer procedures (Release 10) for Evolved Universal Terrestrial Radio Access (E-UTRA), 3GPP TR 36.213 v 10.5.0 (Mar. 2012).
[18] S. Sesia, I. Toufik, M. Baker, LTE–the UMTS long term evolution: from theory to practice, Wiley, 2011.
[19] S. Ramabhadran, J. Pasquale, Stratified round robin: A low complexity packet scheduler with bandwidth fairness and bounded delay, in: Proceedings of the ACM SIGCOMM, 2003, pp. 239–250.
[20] A. Asadi, V. Mancuso, A survey on opportunistic scheduling in wireless communications, IEEE Communications Surveys & Tutorials PP (99) (2013) 1–18.
[21] R. Knopp, P. Humblet, Information capacity and power control in single-cell multiuser communications, in: Proceedings of IEEE ICC, Vol. 1, 1995, pp. 331–335 vol.1.
[22] 3GPP TS 36.321, Rel. 10, LTE; Evolved universal terrestrial radio access (E-UTRA); medium access control (MAC) protocol specification.
URL `http://www.3gpp.org/ftp/Specs/html-info/36321.htm`
[23] A. Gupta, P. Mohapatra, Energy consumption and conservation in WiFi based phones: a measurement-based study, in: Proceedings of IEEE SECON, 2007, pp. 122–131.
[24] V. Visoottiviseth, T. Piroonsith, S. Siwamogsatham, An empirical study on achievable throughputs of IEEE 802.11n devices, in: Proceedings of IEEE WiOPT, 2009, pp. 1–6.
[25] R. Jain, D.-M. Chiu, W. R. Hawe, A quantitative measure of fairness and discrimination for resource allocation in shared computer system, Eastern Research Laboratory, Digital Equipment Corporation, 1984.
[26] Wi-Fi Alliance, Wi-Fi Peer-to-Peer (P2P) Technical Specification v1.1.
URL `www.wi-fi.org/wi-fi-peer-peer-p2p-specification-v11`
[27] C. Cox, An introduction to LTE: LTE, LTE-advanced, SAE and 4G mobile communications, John Wiley & Sons, 2012.
[28] P. Bender, P. Black, M. Grob, R. Padovani, N. Sindhushyana, S. Viterbi, CDMA/HDR: a bandwidth efficient high speed wireless data service for nomadic users, IEEE Communications Magazine 38 (7) (2000) 70–77.

Appendix A. Proofs of propositions

Proof of Proposition 3

In DRONEE-W, each cluster C_n is scheduled with probability w_n. When cluster C_n is selected by the scheduler, its user with the highest SNR is actually scheduled. For each possible MCS k, user $i \in C_n$ is the one experiencing the highest SNR in its cluster with probability $P_h^{(i|k)} = Pr(C_i > Y_i|MCS_i = k)$, $Y_i = \max_{j\in C_n\setminus\{i\}}\{\Gamma_j\}$. Since channels are independent, using the total probability formula yields $P_h^{(i|k)} = \int_0^\infty [1 - F_i(z|MCS_i=k)]\, dF_{Y_i}(z)$. Given that $\pi_k^{(C_n)}$ represents the probability that cluster C_n can be scheduled with the k-th MCS, the result follows by applying again the total probability formula for the discrete set of MCS values. □

Proof of Proposition 4

The proof is similar to the proof of Proposition 3. In DRONEE-M, the scheduled cluster C_n receives all resources S_{tot}, given that the cluster contains the user with the highest SNR in the system. For each possible MCS k, cluster C_n is the one containing the user experiencing the best SNR with probability $P_h^{(C_n|k)} = Pr(X_n > Y_n|MCS_{C_n} = k)$, with $X_n = \max_{j\in C_n}\{\Gamma_j\}$, and $Y_n = \max_{j\notin C_n}\{\Gamma_j\}$. Since channels are independent, using the total probability formula yields $P_h^{(C_n|k)} = \int_0^\infty [1 - F_{X_n}(z|MCS_{C_n}=k)]\, dF_{Y_n}(z)$. Given that $\pi_k^{(C_n)}$ represents the probability that cluster C_n can be scheduled with the k-th MCS, with which the transmitted bits per symbol are b_k, the result follows by applying again the total probability formula for the discrete set of MCS values. □

Proof of Proposition 6

In DRONEE-M, a user is scheduled when it has the highest SNR. Therefore, for each possible MCS k, user i is scheduled with probability $P_h^{(i|k)} = Pr(C_i > Y_i|MCS_i = k)$, with $Y_i = \max_{j\neq i}\{\Gamma_j\}$. Since channels are independent, using the total probability formula yields $P_h^{(i|k)} = \int_0^\infty [1 - F_i(z|MCS_i=k)]\, dF_{Y_i}(z)$. Given that $\pi_k^{(i)}$ represents the probability that user i can be scheduled with the k-th MCS, the result follows by applying the total probability formula for the discrete set of MCS values. □

Proof of Proposition 9

Due to our stationary traffic and channel quality assumptions, the traffic distribution over a scheduling interval is the same as the long term distribution of throughputs within the cluster C_n. Let us denote by δ_i the ratio between the user's throughout $E[T_i]$ and the total cluster throughput $E[T_{C_n}]$. Therefore, the traffic received over WiFi, $R_{rx}^{(i,wifi)}$, is a fraction $1 - \delta_i$ of the traffic transmitted over the LTE interface by user i, which yields Eq. (18)

Similarly, the WiFi transmission data rate $R_{tx}^{(i,wifi)}$ corresponds to a fraction δ_i of all the traffic delivered by LTE from the other cluster members to the base station, when user i is not the cluster head, which yields Eq. (19). □

Proof of Proposition 10

$P_a^{(i)}$ is the sum of two terms: the probability that user i is the cluster head and receives traffic from other cluster members, and the probability that user i is not cluster head and transmits its packets to the cluster head. Since such probabilities can be interpreted as the average fraction of time spent in either in reception or transmission over the WiFi interface, we have the following expression for $P_a^{(i)}$:

$$P_a^{(i)} = (1 - \delta_i)\frac{R_{tx}^{(i,lte)}}{R_{wifi}} + \delta_i \frac{E[T_{C_n}] - R_{tx}^{(i,lte)}}{R_{wifi}}, \qquad \text{(A.1)}$$

which leads to the result. □

Appendix B. Implementation details of RR and PF

As for the throughput of RR and PF, we use the following approach. RR is a simple scheduling method which distributes the available resources equally among all users. RR can distribute resources in a manner that each user receives equal airtime (i.e., *equal time*) or equal throughput (i.e., *equal rate*). In this paper, we use the *equal time* policy because the *equal rate*

policy would drastically reduce the system throughput in the presence of *poor* users. With RR, the throughput of each user only depends on the total number of users in the system, the probability to transmit with a given MCS, and the total amount of resources S_{tot}:

$$E[T_i] = \frac{1}{N} S_{tot} \sum_{k=1}^{M} \pi_k^{(i)} b_k, \quad i \in \{1 \dots N\}, \tag{B.1}$$

where $\pi_k^{(i)}$ values are computed through Eq. (3), and $1/N$ is the probability of any user being scheduled.

PF is a priority-based opportunistic scheduler with fairness constraints. Under PF, scheduling priorities are determined by the ratio of feasible data rate to average throughput at each time instant t (i.e., $R_i(t)/\mu_i(t)$, $\forall i \in \{1 \dots N\}$). In this work, we compare our proposal against PF because of its popularity in the research community and because it has been partially implemented in 3G systems [28]. Unfortunately the majority of analytical models with a closed form expression for throughput of PF does not produce accurate results in scenarios in which data rates do not follow the Shannon capacity formula. Therefore, we use a home grown C++ simulator to evaluate the performance of PF, in which we implement a PF averaging window [28] equal to 100 frames, and schedule only one user per frame.